Microfluid Nanofluid (2013) 14:809–815
DOI 10.1007/s10404-012-1099-z

RESEARCH PAPER

An integrated microfluidic signal generator using multiphase droplet grating

Zhenhua Shen · Yun Zou · Xianfeng Chen

Received: 11 June 2012 / Accepted: 21 September 2012 / Published online: 20 November 2012

Abstract An integrated and reconfigurable optofluidic signal generator based on multiphase droplet grating is demonstrated in this paper. The chip is fabricated with an inexpensive, optically clear and non-toxic silicone elastomer-polydimethylsiloxane (PDMS) by conventional soft lithography. Droplet grating is formed by a stream of plugs which are generated through a typical microfluidic T-junction. Since the refractive indices of the two immiscible liquids are different, the alternative mobility of the plug results in the periodical change of the reflectivity at the fluid/PDMS interface. The real-time tunability in the frequency and amplitude of the signal can be realized by varying the flow rates of the liquids. In experiments, both rectangle and triangle signals are displayed and the signal frequency ranges from 1 to 525 Hz. This signal generator can be easily integrated into other microfluidic networks to create versatile functionalities. Furthermore, we present coding functions based on the signal generator on a chip. Such a signal generator has great potential as a signal source or a part of functionalities for lab-on-a-chip applications.

Keywords Optofluidics · Signal generator · Droplet grating · Microfluidics

Z. Shen · Y. Zou · X. Chen (✉)
Department of Physics, The State Key Laboratory on Fiber Optic Local Area Communication Networks and Advanced Optical Communication Systems, Shanghai Jiao Tong University, Shanghai 200240, China
e-mail: xfchen@sjtu.edu.cn

1 Introduction

The marriage of optics and microfluidics has led to a wide variety of researches in miniaturization and integration of optofluidic components on a chip (Psaltis et al. 2006; Monat et al. 2007; Schmidt and Hawkins 2011). Compared with traditional rigid optical devices, optofluidic elements show unique features due to the nature of the liquids which makes the device highly flexible, reconfigurable and real-time tunable (Nguyen 2010; Li and Psaltis 2007). Integrating all sorts of optical components onto a miniaturized compact chip is one of the ultimate goals of optofluidics, providing significant benefits such as low costs, easy fabrication, less reagent consumption, portability and high degrees of functionalities. To date, various innovative underlying elements of the optofluidic system fabricated through different kinds of microprocessing techniques such as soft lithography (Xia and Whitesides 1998; Duffy et al. 1998), femtosecond laser microprocessing (Sugioka and Cheng 2011, 2012; Osellame et al. 2011) and hot-embossing (Zhang et al. 2008; Abgrall et al. 2007) have mushroomed, including light sources (Yang et al. 2011; Song and Psaltis 2010; Tang et al. 2009; Lee et al. 2011a, b; Aubry et al. 2011; Song et al. 2009), switches (Song and Psaltis 2011b; Lim et al. 2011; Groisman et al. 2008; Seow et al. 2009, 2011), microlenses (Mao et al. 2009; Fei et al. 2011; Song et al. 2010a, b; Huang et al. 2010; Shi et al. 2009), waveguides (Yang et al. 2012; Chung and Erickson 2011; Sun et al. 2007), sensors (Chao et al. 2011; Lapsley et al. 2009; Zhang et al. 2011), cytometers (Cho et al. 2010; Song et al. 2011), interferometers (Chin et al. 2010; Lapsley et al. 2011; Dumais et al. 2008; Song and Psaltis 2011a) and so on (Xiong et al. 2011; Yu et al. 2010; Chin et al. 2008; Zou et al. 2010).

Droplet microfluidics has drawn much attention due to its distinctive properties in compartmentalizing and

performing typical laboratory operations in a nano- and picoliter volume of droplets, offering new routes for chemical sample delivery and analysis (Trivedi et al. 2010; Teh et al. 2008), organic synthesis (DeMello 2006) and microreactors (El-Ali et al. 2006). Microdroplet devices allow small sample volume and fast analysis with high accuracy, repeatability and sensitivity. Thanks to the mature droplet microfluidic techniques, microdroplets can be generated uniformly and periodically and can be manipulated to merge or split according to the requirements (Rosenauer and Vellekoop 2009). In addition, microdroplet systems are able to be utilized to encrypt and decrypt signals (Fuerstman et al. 2007) and perform some simple Boolean logic functions (Prakash and Gershenfeld 2007; Cheow et al. 2007), which show great potential in realization of a microfluidic computer chip. Recently, the fusion of optofluidics and droplet microfluidics has resulted in the emergence of some novel devices, such as tunable long period grating (Chin et al. 2008), Michelson interferometer (Chin et al. 2010), reconfigurable diffraction grating (Yu et al. 2010) and fast-switching dye lasers (Aubry et al. 2011; Tang et al. 2009). However, the signal sources used for microfluidic chip experiments are mainly external bulky commercial devices (Song and Psaltis 2011b; Bransky et al. 2009), although useful, can limit the portability and convenience. The study of the signal generator that can be readily integrated into other microfluidic network is desirable.

In this paper, we introduce an optofluidic signal generator based on multiphase droplet grating. Breakup of the two immiscible liquids at the T-junction produces plugs. When the flow rates of the immiscible fluids are fixed, the droplet grating is formed by a stream of plugs with a steady period. Alternative of the aqueous phase and oil phase results in the periodical change of the refractive index (RI) as well as the reflectivity at the fluid/PDMS interface. The main advantages of this signal generator are as follows. First, in contrast to the signal generator based on complex electronic circuits, it will not be influenced by electromagnetic interference. Second, signal can be generated without the limitation of wavelength from near-infrared to near-ultraviolet owing to the optical transparency of PDMS. Last but not least, it is simple to fabricate and can be easily integrated onto a microfluidic chip as a part of functionalities in microfluidic systems. Based on this signal generator, we further demonstrate a compact and reconfigurable optical device for information coding on a chip.

2 Design and working principle

Figure 1a presents the schematic of the signal generator, which consists of the T-junction microchannel, two PDMS-air lenses and fiber ports. The micochannel in the grating region is 125 μm in width, the radius of the PDMS-air lens is 155 μm and all features are 128 μm in height as depicted in Fig. 1b. Since the outer diameter of the step index multimode optical fiber (core diameter = 50 μm, outer diameter = 125 μm, numerical aperture (NA) = 0.22, Thorlabs) is 125 μm, the fiber port is designed to have a width of 128 μm, which is slightly larger than the width of the fiber as shown in Fig. 1c. The incident angle was designed to be 62°. According to the Fresnel equations of reflection, the incident angle affects the optical reflection at the PMDS/fluid interface and thus leads to the altering of the amplitude of the signal. However, the signal shapes and frequencies discussed in the paper will not be influenced. The integrated PDMS-air microlenses are used to compensate the divergence of the light due to the NA of the multimode fiber. In the formation of the droplet grating, the silicone oil (viscosity = 10 centistokes, $RI = 1.399$, Dow Corning) is used as the carrier fluid while the de-ionized (DI) water ($RI = 1.333$) serves as the dispersed liquid for droplets. When the dispersed fluid comes into the main channel, it blocks the flow of the continuous fluid and the pressure is built up. Finally, the high resistance at the T-junction breaks the dispersed fluid and forms a plug. As this process repeats, the droplet grating is formed by a series of plugs with a steady period. Due to the alternative of the aqueous phase and oil phase, the refractive index as well as the reflectivity at the fluid/PDMS interface changes periodically. The grating period can be tuned by varying the flow rates of the fluids. When the flow rates of the liquids are low, the input light beam size at the fluid/PDMS interface is smaller than the length of the plug and the rectangle signal is performed as shown in Fig. 2a. Otherwise, the triangle waveform can be demonstrated as depicted in Fig. 2b. In experiments, two kinds of liquids we employed are silicone oil and DI water, whose refractive indices are 1.399 and 1.333, respectively. Since the refractive index of the silicone oil is almost the same as that of PDMS (RI = 1.412), the input light barely reflects and thus contributes to the valley of the signal. Conversely, the reflection caused by the PDMS/DI water interface leads to the peak of the waveform.

3 Fabrication processes and experimental setup

Two different kinds of chips were fabricated with an optical clear silicone elastomer (PDMS) by soft lithography. One is the signal generator using multiphase droplet grating, and the other is an information coding device by integrating the signal generator with other microfluidic networks. Although showing different functionalities, both chips have the same fabrication processes as follows:

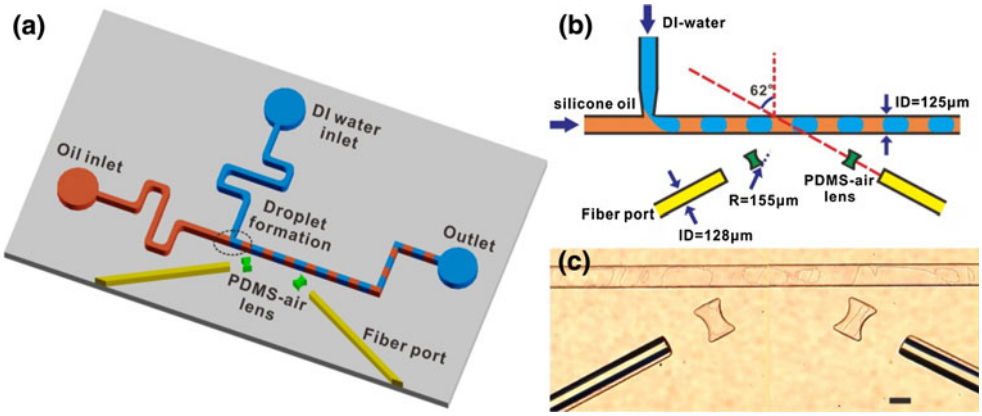

Fig. 1 **a** Schematic of the optofluidic signal generator. **b** Top view of the structure of the signal generator. **c** Microscope image of the device with inserted multimode optical fibers. (*Scale bar*: 125 μm)

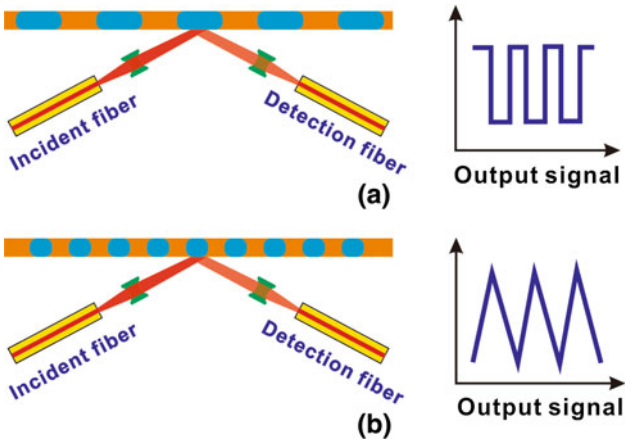

Fig. 2 Illustration of different kinds of signal generation **a** rectangle signal generation when the beam size is smaller than the length of the plug. **b** Triangle signal generation when the beam size is larger than the length of the plug

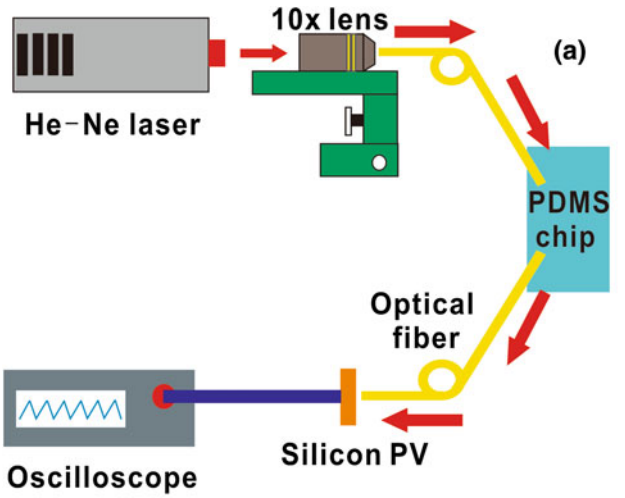

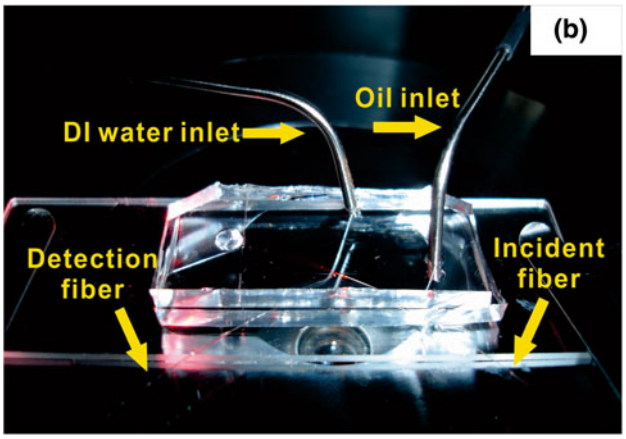

Fig. 3 **a** Schematic illustration of the experimental setup, the *red arrows* indicate the directions of light propagation. **b** An optofluidic chip under experiment

The micro-channel structure was first designed with AutoCAD (Autodesk) and then transferred to high-resolution photomasks fabricated on transparencies. Next, the 3-inch silicon wafer was spin-coated with 128-μm thick layer of the negative photoresist SU-8 (MicroChem) and patterned utilizing a MA6 mask aligner (Suss MicroTec). Then the wafer was developed for 10 min and an IPA rinse was performed to finish the development process. Finally, a nanoscale thick layer of chromium copper was sputtered to the surface to confirm the completion of the mold fabrication process. A 4-mm thick layer of PDMS prepolymer (base and its curing agent mixed at the weight ratio of 10:1, Sylgard 184, Dow Corning) was cast to the SU-8 mold and put under vacuum for about 45 min to remove all the air bubbles. After baking for 2 h at 60 °C in an oven, the PDMS cast was peeled off from the mold. The structured PMDS slice was bonded with a flat PDMS piece after oxygen plasma treatment by a plasma cleaner (PDC-002, Harrick Plasma) for 90 s and the surface properties of PDMS would be changed from hydrophobicity to hydrophilicity. At last, the chip was baked at 80 °C in an oven for at least 2 h to ensure the bonding effect. Since the carrier fluid we employed is silicon oil which is hydrophobic, it is necessary for the microchannel to regain hydrophobicity to form a steady droplet grating. Otherwise,

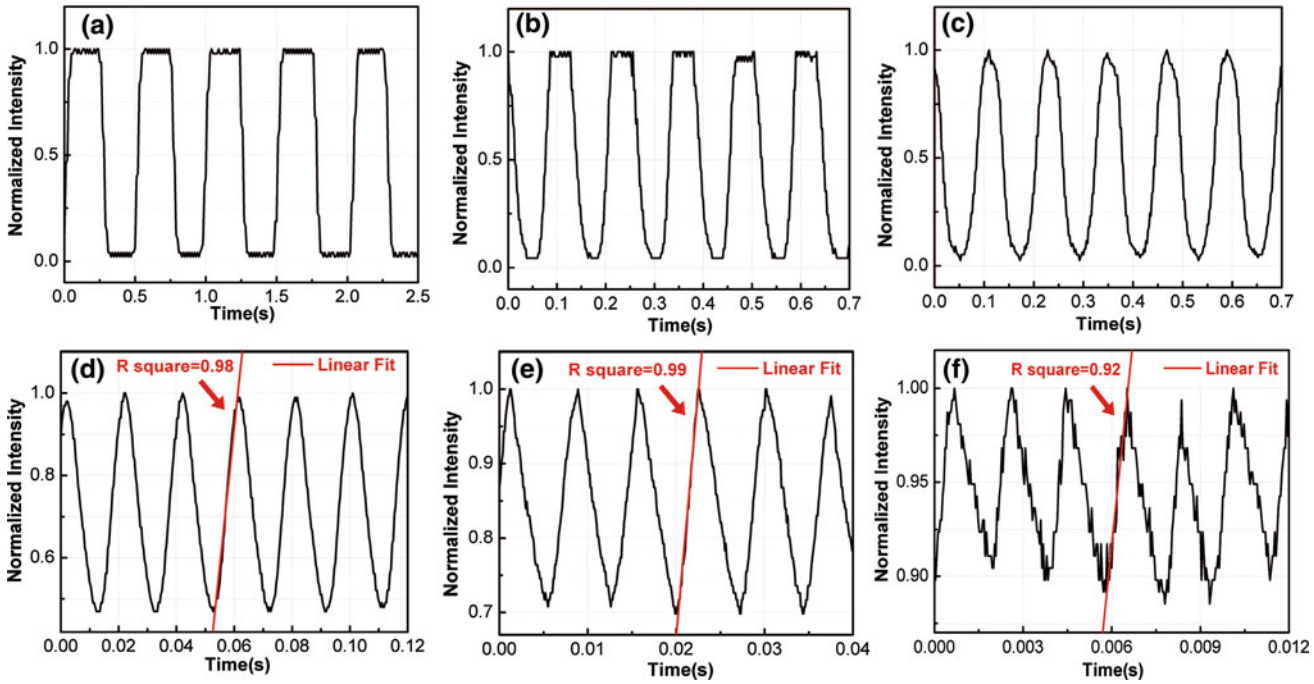

Fig. 4 Output waveforms at different flow rates of DI water and silicone oil. **a** $Q_{oil} = Q_{water} = 2$ μL min^{-1}. **b** $Q_{oil} = Q_{water} = 4$ μL min^{-1}. **c** $Q_{oil} = Q_{water} = 5$ μL min^{-1}.**d** $Q_{oil} = Q_{water} = 15$ μL min^{-1}. **e** $Q_{oil} = Q_{water} = 30$ μL min^{-1}. **f** $Q_{oil} = Q_{water} = 60$ μL min^{-1}. *Red lines* show linear fits for half period of the triangle signals, the R^2 values represent good linearity of the triangle waveforms

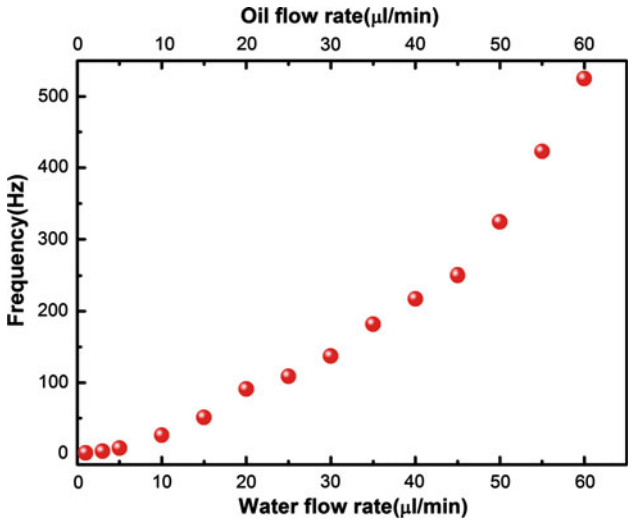

Fig. 5 The tuning of the signal frequency versus the flow rates of silicone oil and DI water

the droplet formation process would be unstable. So finally the fabricated PDMS chip should be stored about 2 days before conducting the experiment, which helped the microchannel regain hydrophobicity.

Figure 3a gives a schematic illustration of the experimental setup. Two multimode fibers were inserted into the fiber channel as the input and output of the chip. The optical fibers were cut by a high-precision cleaver to achieve 90° surface for minimizing the optical coupling loss. We dipped the fiber into the silicon oil which was employed as an excellent lubricant before the fiber insertion to prevent the fiber from being broken. In order to investigate the performance of the optofluidic signal generator, a He–Ne laser with a center wavelength of 632.8 nm was coupled into the optical fiber as the input by using a five-dimensional adjustment of racks and lifts as a coupling device. The output signal was detected by a silicon photovoltaic cell which directly connected to an oscilloscope (DS1202CA, Rigol Technologies Inc.). After the incident light reflected at the PDMS-liquid interface, the light signal finally reached the output fiber and showed up on the oscilloscope through the photoelectric conversion by the silicon photovoltaic cell. During the propagation of the light, a pair of PDMS-air lenses was designed to focus the light and compensate the divergence. The silicone oil and DI water were injected into the chip using syringe pumps (PHD2000, Harvard Apparatus). To get a clear version of the microchannel in the experiments, the chip was observed under an inverted microscope (IX51, Olympus). The photograph of the chip on the microscope system is shown in Fig. 3b.

4 Results and discussion

To get a signal with a duty cycle of 0.5, the flow rate ratio between the silicone oil and DI water was fixed at 1. When

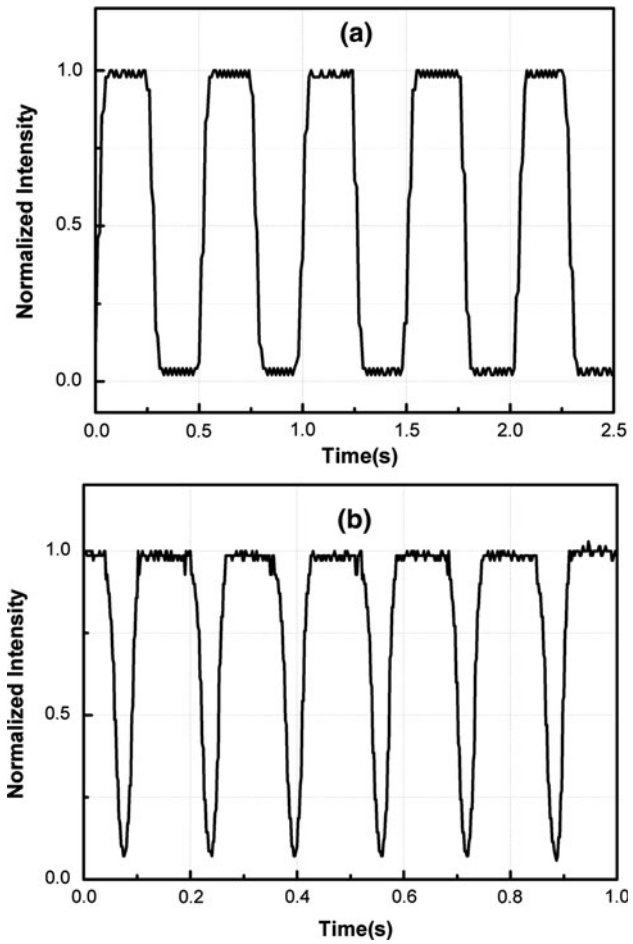

Fig. 6 Different kinds of signal with fixed flow rate of silicone oil at 2 μL min^{-1}, **a** Q_{water} = 2 μL min^{-1} with an output of rectangle waveform. **b** Q_{water} = 5 μL min^{-1} with an output of pulse signal waveform

the flow rates were 2 μL min^{-1}, a stable rectangle waveform with a frequency of 2 Hz was formed as is shown in Fig. 4a. As the flow rates gradually increased, the rectangle signal transformed to trapezoid and finally became triangle as depicted in Fig. 4b, c. Figure 4c presents a critical waveform from trapezoid to triangle at the flow rates of 5 μL min^{-1}, which means the beam size of the light was just the same as the length of plug. As the flow rates continued to increase, although the signal remained to be triangle, the contrast ratio between the peak and the valley of the signal became smaller and smaller due to the decrease of the grating period. Figure 4d–f shows the triangle signal with frequencies ranging from 51 to 525 Hz. The triangle signals presented good linearity and a maximum frequency of 525 Hz was achieved at the flow rates of 60 μL min^{-1}. Beyond this frequency the droplet grating stream was unstable and jets occurred. In the experiment, it would take several seconds to form a new stable liquid grating from the original one by changing the flow rates of the liquids. The linear fit curve and the R square value were fitted and calculated in OriginPro 8.0. Figure 5 shows the signal frequency versus the flow rates of the two immiscible fluids. If the grating period was independent of the flow rates of the liquids, the signal frequency should have been linear with the flow rates of the liquids. The nonlinearity of the data was caused by the decrease of the grating period as the flow rates grew up. Figure 6a shows regular rectangle waveforms when the flow rates of the silicone oil and DI water are both 2 μL min^{-1}. Fixing the flow rates of silicone oil at 2 μL min^{-1} and increasing the flow rate of DI water to 5 μL min^{-1}, the waveform turned out to be pulse signals as shown in Fig 6b. Signals with higher

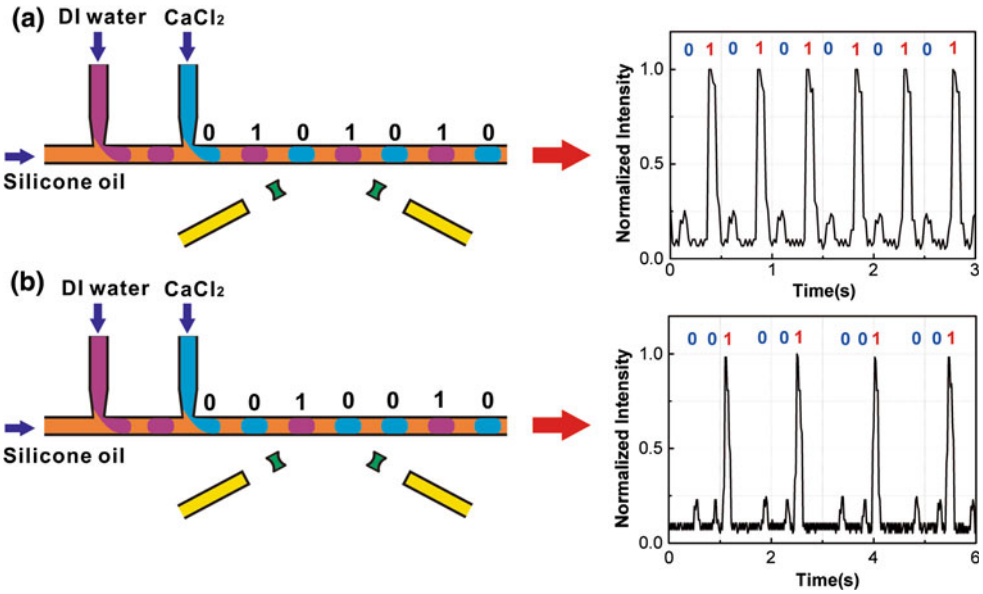

Fig. 7 Schematic diagrams and experiment results for different types of coding.
a 0101…coding at the flow rates of Q_{oil} = 1.5 μL min^{-1}, Q_{water} = 1.0 μL min^{-1} and Q_{CaCl2} = 0.7 μL min^{-1}.
b 001001…coding at the flow rates of Q_{oil} = 3.0 μL min^{-1}, Q_{water} = 0.4 μL min^{-1} and Q_{CaCl2} = 0.6 μL min^{-1}

frequencies and larger contrast ratios can be achieved using two opposing T-junctions (Tang et al. 2009) and minimizing the beam size at the PDMS/liquid interface, which will further enhance the performance of the device.

5 Information coding device on a chip

We present a simple and reconfigurable information coding device as an example for applications by integrating the signal generator with another T-junction structure. The information coding chip mainly consists of double T-junctions, a pair of PDMS lenses and two fiber ports. In experiment, the experimental setup was almost the same as that of the signal generator. Here the additional aqueous phase liquid we used for the new inlet was 1.75 M $CaCl_2$ aqueous solution with a refractive index of 1.373. The DI water droplets and $CaCl_2$ droplets dispersed in the silicone oil contributed to the higher and lower peaks of the signal, respectively. By defining the signal peaks generated by the $CaCl_2$ droplet and DI water droplet as 0 and 1, a stable 01 type of signal was formed at the flow rates of $Q_{oil} = 1.5$ μL min^{-1}, $Q_{water} = 1.0$ μL min^{-1} and $Q_{CaCl_2} = 0.7$ μL min^{-1} as shown in Fig. 7a. By carefully changing the flow rate of the silicone oil and the ratio between DI water and $CaCl_2$ solution, a stable 001 type of signal was established when the flow rates of the liquids were $Q_{oil} = 3.0$ μL min^{-1}, $Q_{water} = 0.4$ μL min^{-1} and $Q_{CaCl_2} = 0.6$ μL min^{-1}, respectively, which is depicted in Fig. 7b. In addition, more types of information coding can be achieved via programmable syringe pumps and more T-junction structures integrated on a chip. The former method provides more accurate control of the droplet formation with time evolution while the latter increases the droplet types and numbers. Both of the two methods would lead to versatile kinds of information coding.

6 Conclusion

In summary, we report the first optofluidic signal generator which is incorporated into a PDMS chip. Different types of signal including rectangle and triangle waveforms have been demonstrated. Waveform and frequency of the signal are realized by adjusting the flow rates of two immiscible fluids. The high linearity of the triangle waveforms shows great potential in on-chip biochemical sensing applications. The convenience in fabrication and operation not only paves the way for on-chip signal generation, but also opens the door to integration with other microfluidic networks. In particular, we also demonstrated a reconfigurable and tunable optofluidic information coding device. We believe that the fusion of this compact and tunable signal generator with a wide range of state-of-the-art optofluidic elements can create much more functionalities on a chip.

Acknowledgments This research was supported by the National Natural Science Foundation of China (Grant No. 61125503) and the Foundation for Development of Science and Technology of Shanghai (Grant No. 11XD1402600, No. 10JC1407200).

References

Abgrall P, Low LN, Nguyen NT (2007) Fabrication of planar nanofluidic channels in a thermoplastic by hot-embossing and thermal bonding. Lab Chip 7(4):520–522. doi:10.1039/b616134k

Aubry G, Kou Q, Soto-Velasco J, Wang C, Meance S, He JJ, Haghiri-Gosnet AM (2011) A multicolor microfluidic droplet dye laser with single mode emission. Appl Phys Lett 98(11):111111. doi:10.1063/1.3565242

Bransky A, Korin N, Khoury M, Levenberg S (2009) A microfluidic droplet generator based on a piezoelectric actuator. Lab Chip 9(4):516–520. doi:10.1039/B814810d

Chao K-S, Lin T-Y, Yang R-J (2011) Two optofluidic devices for the refractive index measurement of small volume of fluids. Microfluid Nanofluid 12(5):697–704. doi:10.1007/s10404-011-0915-1

Cheow LF, Yobas L, Kwong DL (2007) Digital microfluidics: droplet based logic gates. Appl Phys Lett 90(5):054107. doi:Artn054107

Chin LK, Liu AQ, Zhang JB, Lim CS, Soh YC (2008) An on-chip liquid tunable grating using multiphase droplet microfluidics. Appl Phys Lett 93(16):164107. doi:10.1063/1.3009560

Chin LK, Liu AQ, Soh YC, Lim CS, Lin CL (2010) A reconfigurable optofluidic Michelson interferometer using tunable droplet grating. Lab Chip 10(8):1072–1078. doi:10.1039/b920412a

Cho SH, Godin JM, Chen CH, Qiao W, Lee H, Lo YH (2010) Review Article: recent advancements in optofluidic flow cytometer. Biomicrofluidics 4(4):43001. doi:10.1063/1.3511706

Chung AJ, Erickson D (2011) Optofluidic waveguides for reconfigurable photonic systems. Opt Express 19(9):8602–8609

DeMello AJ (2006) Control and detection of chemical reactions in microfluidic systems. Nature 442(7101):394–402. doi:10.1038/nature05062

Duffy DC, McDonald JC, Schueller OJA, Whitesides GM (1998) Rapid prototyping of microfluidic systems in poly(dimethylsiloxane). Anal Chem 70(23):4974–4984

Dumais P, Callender CL, Noad JP, Ledderhof CJ (2008) Integrated optical sensor using a liquid-core waveguide in a Mach-Zehnder interferometer. Opt Express 16(22):18164–18172

El-Ali J, Sorger PK, Jensen KF (2006) Cells on chips. Nature 442(7101):403–411. doi:10.1038/Nature05063

Fei P, He Z, Zheng C, Chen T, Men Y, Huang Y (2011) Discretely tunable optofluidic compound microlenses. Lab Chip 11(17):2835–2841. doi:10.1039/c1lc20425d

Fuerstman MJ, Garstecki P, Whitesides GM (2007) Coding/decoding and reversibility of droplet trains in microfluidic networks. Science 315(5813):828–832. doi:10.1126/science.1134514

Groisman A, Zamek S, Campbell K, Pang L, Levy U, Fainman Y (2008) Optofluidic 1 × 4 switch. Opt Express 16(18):13499–13508

Huang H, Mao X, Lin SC, Kiraly B, Huang Y, Huang TJ (2010) Tunable two-dimensional liquid gradient refractive index (L-GRIN) lens for variable light focusing. Lab Chip 10(18):2387–2393. doi:10.1039/c005071g

Lapsley MI, Lin S-CS, Mao X, Huang TJ (2009) An in-plane, variable optical attenuator using a fluid-based tunable reflective interface. Appl Phys Lett 95(8):083507. doi:10.1063/1.3213348

Lapsley MI, Chiang IK, Zheng YB, Ding X, Mao X, Huang TJ (2011) A single-layer, planar, optofluidic Mach-Zehnder interferometer for label-free detection. Lab Chip 11(10):1795–1800. doi:10.1039/c0lc00707b

Lee W, Li H, Suter JD, Reddy K, Sun Y, Fan X (2011a) Tunable single mode lasing from an on-chip optofluidic ring resonator laser. Appl Phys Lett 98(6):061103. doi:10.1063/1.3554362

Lee W, Luo YH, Zhu QR, Fan XD (2011b) Versatile optofluidic ring resonator lasers based on microdroplets. Opt Express 19(20): 19668–19674

Li Z, Psaltis D (2007) Optofluidic dye lasers. Microfluid Nanofluid 4(1–2):145–158. doi:10.1007/s10404-007-0225-9

Lim JM, Urbanski JP, Thorsen T, Yang SM (2011) Pneumatic control of a liquid-core/liquid-cladding waveguide as the basis for an optofluidic switch. Appl Phys Lett 98(4):044101. doi:Artn 044101

Mao X, Lin SC, Lapsley MI, Shi J, Juluri BK, Huang TJ (2009) Tunable liquid gradient refractive index (L-GRIN) lens with two degrees of freedom. Lab Chip 9(14):2050–2058. doi:10.1039/b822982a

Monat C, Domachuk P, Eggleton BJ (2007) Integrated optofluidics: a new river of light. Nat Photonics 1(2):106–114. doi:10.1038/nphoton.2006.96

Nguyen NT (2010) Micro-optofluidic Lenses: a review. Biomicrofluidics 4(3):031501. doi:10.1063/1.3460392

Osellame R, Hoekstra HJWM, Cerullo G, Pollnau M (2011) Femtosecond laser microstructuring: an enabling tool for optofluidic lab-on-chips. Laser Photonics Rev 5(3):442–463. doi:10.1002/lpor.201000031

Prakash M, Gershenfeld N (2007) Microfluidic bubble logic. Science 315(5813):832–835. doi:10.1126/science.1136907

Psaltis D, Quake SR, Yang C (2006) Developing optofluidic technology through the fusion of microfluidics and optics. Nature 442(7101):381–386. doi:10.1038/nature05060

Rosenauer M, Vellekoop MJ (2009) 3D fluidic lens shaping–a multiconvex hydrodynamically adjustable optofluidic microlens. Lab Chip 9(8):1040–1042. doi:10.1039/b822981c

Schmidt H, Hawkins AR (2011) The photonic integration of non-solid media using optofluidics. Nat Photonics 5(10):598–604. doi:10.1038/Nphoton.2011.163

Seow YC, Lim SP, Lee HP (2009) Tunable optofluidic switch via hydrodynamic control of laminar flow rate. Appl Phys Lett 95(11):114105. doi:10.1063/1.3229887

Seow YC, Lim SP, Lee HP (2011) Micro-light distribution system via optofluidic cascading prisms. Microfluid Nanofluid 11(4): 451–458. doi:10.1007/s10404-011-0810-9

Shi J, Stratton Z, Lin S-CS, Huang H, Huang TJ (2009) Tunable optofluidic microlens through active pressure control of an air–liquid interface. Microfluid Nanofluid 9(2–3):313–318. doi:10.1007/s10404-009-0548-9

Song W, Psaltis D (2010) Pneumatically tunable optofluidic dye laser. Appl Phys Lett 96(8):081101. doi:10.1063/1.3324885

Song W, Psaltis D (2011a) Optofluidic membrane interferometer: an imaging method for measuring microfluidic pressure and flow rate simultaneously on a chip. Biomicrofluidics 5(4):044110. doi:10.1063/1.3664693

Song W, Psaltis D (2011b) Pneumatically tunable optofluidic 2 × 2 switch for reconfigurable optical circuit. Lab Chip 11(14): 2397–2402. doi:10.1039/c1lc20220k

Song W, Vasdekis AE, Li Z, Psaltis D (2009) Low-order distributed feedback optofluidic dye laser with reduced threshold. Appl Phys Lett 94(5):051117. doi:10.1063/1.3079799

Song C, Nguyen N-T, Tan S-H, Asundi AK (2010a) A tuneable micro-optofluidic biconvex lens with mathematically predictable focal length. Microfluid Nanofluid 9(4–5):889–896. doi:10.1007/s10404-010-0608-1

Song C, Nguyen N-T, Yap YF, Luong T-D, Asundi AK (2010b) Multi-functional, optofluidic, in-plane, bi-concave lens: tuning light beam from focused to divergent. Microfluid Nanofluid 10(3):671–678. doi:10.1007/s10404-010-0703-3

Song CL, Luong TD, Kong TF, Nguyen NT, Asundi AK (2011) Disposable flow cytometer with high efficiency in particle counting and sizing using an optofluidic lens. Opt Lett 36(5):657–659

Sugioka K, Cheng Y (2011) Integrated microchips for biological analysis fabricated by femtosecond laser direct writing. MRS Bull 36(12):1020–1027. doi:10.1557/mrs.2011.274

Sugioka K, Cheng Y (2012) Femtosecond laser processing for optofluidic fabrication. Lab Chip 12(19):3576–3589. doi:10.1039/c2lc40366h

Sun HY, He F, Zhou ZH, Cheng Y, Xu ZZ, Sugioka K, Midorikawa K (2007) Fabrication of microfluidic optical waveguides on glass chips with femtosecond laser pulses. Opt Lett 32(11):1536–1538

Tang SK, Li Z, Abate AR, Agresti JJ, Weitz DA, Psaltis D, Whitesides GM (2009) A multi-color fast-switching microfluidic droplet dye laser. Lab Chip 9(19):2767–2771. doi:10.1039/b914066b

Teh SY, Lin R, Hung LH, Lee AP (2008) Droplet microfluidics. Lab Chip 8(2):198–220. doi:10.1039/b715524g

Trivedi V, Doshi A, Kurup GK, Ereifej E, Vandevord PJ, Basu AS (2010) A modular approach for the generation, storage, mixing, and detection of droplet libraries for high throughput screening. Lab Chip 10(18):2433–2442. doi:10.1039/C004768f

Xia YN, Whitesides GM (1998) Soft lithography. Annu Rev Mater Sci 28:153–184

Xiong S, Liu AQ, Chin LK, Yang Y (2011) An optofluidic prism tuned by two laminar flows. Lab Chip 11(11):1864–1869. doi:10.1039/c1lc20180h

Yang Y, Liu AQ, Lei L, Chin LK, Ohl CD, Wang QJ, Yoon HS (2011) A tunable 3D optofluidic waveguide dye laser via two centrifugal Dean flow streams. Lab Chip 11(18):3182–3187. doi:10.1039/c1lc20435a

Yang Y, Liu AQ, Chin LK, Zhang XM, Tsai DP, Lin CL, Lu C, Wang GP, Zheludev NI (2012) Optofluidic waveguide as a transformation optics device for lightwave bending and manipulation. Nat Commun 3:651. doi:10.1038/ncomms1662

Yu JQ, Yang Y, Liu AQ, Chin LK, Zhang XM (2010) Microfluidic droplet grating for reconfigurable optical diffraction. Opt Lett 35(11):1890–1892

Zhang L, Gu F, Tong L, Yin X (2008) Simple and cost-effective fabrication of two-dimensional plastic nanochannels from silica nanowire templates. Microfluid Nanofluid 5(6):727–732. doi:10.1007/s10404-008-0314-4

Zhang XW, Ren LQ, Wu X, Li H, Liu LY, Xu L (2011) Coupled optofluidic ring laser for ultrahigh-sensitive sensing. Opt Express 19(22):22242–22247

Zou Y, Liu K, Shen Z, Chen X (2010) Magnetic-fluid core optical fiber. Microfluid Nanofluid 10(2):447–451. doi:10.1007/s10404-010-0665-5